CrossMark

RESEARCH PAPER

Comparisons of the nanoparticle emission characteristics between GDI and PFI vehicles

Jihwan Jang · Jongtae Lee · Jeongsoo Kim · Sungwook Park

Abstract To compare the particle emissions of gasoline direct injection (GDI) and port fuel injection (PFI) vehicles in this study, the particulate matter of exhaust emissions was sampled from a constant volume sampler tunnel and tailpipe using a chassis dynamometer. Using the gravimetric method and a condensation particle counter, the particulate matter mass (PM) and particle number (PN) of the particle size according to the current regulations were measured. Nanometer-sized particle emissions, which are smaller than regulated particle emissions, were measured by an engine exhaust particle sizer. Four test vehicles, which included two GDI vehicles and two PFI vehicles, were tested in various driving modes. The test results show that the particle emissions from the GDI vehicles were higher than the particle emissions from the PFI vehicles. In addition, the test vehicles had the highest emissions in cold start conditions. In the GDI vehicles, the PM and PN satisfied the current regulations but PN did not satisfy the EURO 6c regulations that will be implemented in 2017. In all driving modes, the particle size distribution show that the most common particle size was approximately 50 nm, and the results according to the driving patterns of each mode were confirmed.

Abbreviations

GDI	Gasoline direct injection
PFI	Port fuel injection
PM	Particulate matter mass
PN	Particle number
LEV	Low emission vehicle
PMP	Particle measurement program
CVS	Constant volume sampler
CPC	Condensation particle counter
VPR	Volatile particle remover
HEPA	High-efficiency particulate air
EEPS	Engine exhaust particle sizer
SMPS	Scanning mobility particle sizer
DMS	Differential mobility spectrometer
ELPI	Electrical low pressure impactor
FTP	Federal test procedure
NEDC	New european driving cycle
UDC	Urban driving cycle
EUDC	Extra urban driving cycle

J. Jang
Graduate School of Hanyang University, Seoul 133-791, Korea

J. Lee · J. Kim
National Institute of Environmental Research, Incheon 404-708, Korea

S. Park (✉)
School of Mechanical Engineering, Hanyang University, 222 Wangsimni-ro, Seongdong-gu, Seoul 133-791, Korea
e-mail: parks@hanyang.ac.kr

NIER   National Institute of Environmental
        Research
DPF   Diesel particle filter

Introduction

Over the years, there have been many advances in gasoline vehicles. Specifically, the gasoline engine was developed to complement the shortcomings of the port fuel injection (PFI) engine, including changes to the fuel injection system, turbocharger, and variable valve control (Lee and Yeom 2012; Pesiridis 2012; Zhao et al. 1999). These advances, in turn, led to improved engine efficiency. In particular, the new fuel injection system of the gasoline direct injection (GDI) engine has major advantages such as output improvement, fuel efficiency, and fuel injection control. In addition, the direct injection of the GDI engine causes a charge cooling effect, which leads to higher volumetric efficiency and an increased compression ratio. As well as, the fuel efficiency of the GDI engine is improved as precise fuel injection is possible (Bonatesta et al. 2014; Brehob et al. 1998). For this reason, GDI vehicles are increasingly common in the automotive industry, and GDI vehicles may replace conventional PFI vehicles. However, despite these advantages, the problem of particle emissions from GDI engines has been confirmed. Furthermore, as serious atmospheric pollution problems and their adverse effects on humans have become growing concerns, the particle emission problem of GDI engines has become a serious issue throughout the world. (Brugge et al. 2007; Künzli et al. 2000). To solve this problem, emission regulations for vehicles have become increasingly strict. In particular, regulations for GDI vehicle particle emissions have become more stringent. In the past, Europe only had particle emission standards for diesel vehicles. However, starting in 2009, the PM emission standard for GDI vehicles was legislated and PN regulations for GDI vehicle were enacted in 2014. Particle emission standard of the EURO-6c to be implemented in 2017 regulates PM and PN emissions at the same levels as for diesel vehicles ((EC) No 715/2007 2007). Even in the U.S., the interest in particle emissions from GDI vehicles has been increasing. Starting in 2008, the California Low Emission Vehicle II (LEV II) standards were adopted, which include a PM standard of 0.010 g/mi that applies to both GDI and Diesel vehicles. Particle emissions from GDI vehicles have become bigger issues because of the increase in GDI vehicles.

According to these strengthened regulations, research institutes have actively researched particle emissions from GDI vehicles. Previous study stated that GDI vehicles emit more particulate matter and have higher particle numbers than PFI vehicles and diesel vehicles equipped with diesel particle filters (DPFs) (Braisher et al. 2010). Also, partially fuel-rich zones, fuel spray impingement, and wall wetting in the combustion chamber are caused by the fuel injection system of GDI vehicles (Cavina et al. 2015; Luijten et al. 2013), so more incomplete combustion occurs (Bonandrini et al. 2012; Maricq et al. 1999; Sementa 2012). As a result, GDI vehicles emit more PM and PN than PFI engines.

In recent years, nanometer-sized particle emissions, which are smaller than regulated particle emissions, have become a controversial subject. Nanoparticle emissions are known to cause more adverse health effects than regulated particle emissions because of the greater surface area per unit volume of the particles (Donaldson et al. 2000; Nel et al. 2006). Many studies have been done to measure nanoparticle emissions using different types of measurement equipment (Arsie et al. 2011; Kayes and Hochgreb 1998; Zhang and McMahon 2012). Some work measured and compared nanoparticle emissions under the NEDC mode using scanning mobility particle sizer (SMPS), differential mobility spectrometer (DMS), electrical low pressure impactor (ELPI), and engine exhaust particle sizer (EEPS) (Rubino et al. 2005). The study stated that SMPS is more suitable for steady-state measurement than ELPI. In the case of transients, DMS and EEPS are more appropriate and also respond much faster than ELPI. In addition, the effect of nanoparticle emissions on various driving modes and the regulated emission characteristics of four types of vehicles (PFI gasoline, DPF diesel, non-DPF diesel, and LPG) have been studied. (Kim et al. 2013). Almost all of the particles from the test vehicles were emitted during the cold start modes. One of the major causes of particle emission generation is the warming up of the engine. Most of the soot is formed in the inhomogeneous mixture combustion process under a cold start

condition (Fu et al. 2014; Price et al. 2007; Tong et al. 2001).

Many studies have shown particle emissions of vehicles, but analysis of particle emissions emitted from gasoline vehicles is lacking. Therefore, this study was conducted to compare the particle emission characteristics of GDI and PFI vehicles. The purpose of this study is to confirm the regulated and nanoparticle emissions of test vehicles and to analyze the emission characteristics under various conditions, such as the driving mode, driving patterns, and temperature conditions on starting the engine. To compare the characteristics in various conditions, the federal test procedure-75 (FTP-75) and new european driving cycle (NEDC) driving modes were tested as the emission certification modes of the U.S and Europe, and the national institute environment research (NIER) number 6 and 9 modes were tested to reflect driving in Korea. EEPS equipment was used to measure the nanoparticles in accordance with the findings of the Joint Research Centre in Europe (Jon Andersson et al. 2007). This apparatus can determine the number of emissions and the size distributions of the particles in the range from 5.6 to 560 nm.

Experimental setup and procedure

Test vehicles and driving conditions

In this study, four test vehicles were tested on a chassis dynamometer summarized in Table 1 to evaluate the regulated PM, PN, and PN concentration under the FTP-75, NEDC, NIER06, and NIER09 driving modes. Of the four test vehicles, two were equipped with GDI engines and two were equipped with PFI engines. The detailed specifications of the four test vehicles are given in Table 2. In order to compare the particle emissions from GDI and PFI vehicles under the same conditions, one 2.0L engine equipped with a Turbocharged GDI system and one conventional PFI system, respectively, were used. The remaining two vehicles were equipped with 1.6L GDI and PFI systems.

The FTP-75, NEDC, NIER06, and NIER09 driving modes were chosen to compare the characteristics of particle emissions from the test vehicles in various driving conditions. The FTP-75 U.S. certification test mode consists of a transient cycle of a cold start condition, stabilized cycle, a soaking phase with the engine off and a transient cycle of a hot start condition, in that order. The average and maximum speeds of the FTP-75 mode are 34.2 and 91.2 km/h, respectively. In addition, the driving time and distance of the FTP-75 mode are 1874 s and 17.77 km, respectively. In NEDC mode, the entire cycle consists of four ECE-15 urban driving cycles (UDC) of urban driving conditions and one extra urban driving cycle (EUDC) including a high speed of 120 km/h, and an average speed, driving time, and distance of 33.6 km/h, 1180 s, and 11.01 km, respectively. The NIER06 and NIER09 non-certified test modes proposed by the National Institute of Environmental Research (NIER) were designed considering the city driving tendencies in Korea, and consist of only one phase each. The average and maximum speeds of the NIER modes are not higher than those of the certification test modes in the US and Europe, because they only simulate urban driving. The characteristics of the driving modes for this study are shown in Table 3, and the vehicle speed profiles for NIER06 and NIER09 are shown in Fig. 1.

Table 1 Specification of chassis dynamometer	Items	Specifications
	Model	AVL chassis dynamometer 48 compact
	Maximum speed	200 km/h
	Maximum force	10,096 N
	Maximum calibration force	8000 N
	Measured base interia	1610 kg
	Minimum specified interia	454 kg
	Maximum specified interia	5443 kg
	Roller-diameter	1219.2 mm
	Encoder pulses	10,000

Table 2 Specifications of four types of test vehicles using chassis dynamometer test

Specifications	2.0 T-GDI	2.0 PFI	1.6 GDI	1.6 PFI
Empty vehicle weight (kg)	1520	1415	1190	1187
Engine displacement (cc)	1999	1999	1591	1592
Max. power (PS)	271	165	124	140
Max. torque (kg m)	37.2	20.2	15.9	17.0
Number of cylinders (−)	4	4	4	4

Table 3 Characteristics of test driving modes

Driving mode	Average speed (km/h)	Maximum speed (km/h)	Driving time (s)	Driving distance (km)	Start condition (−)
FTP-75	34.2	91.2	1874	17.77	Cold
NEDC	33.6	120	1180	11.01	Cold
NIER06	19.5	60.1	846	4.89	Hot
NIER09	34.1	70.9	926	8.8	Hot
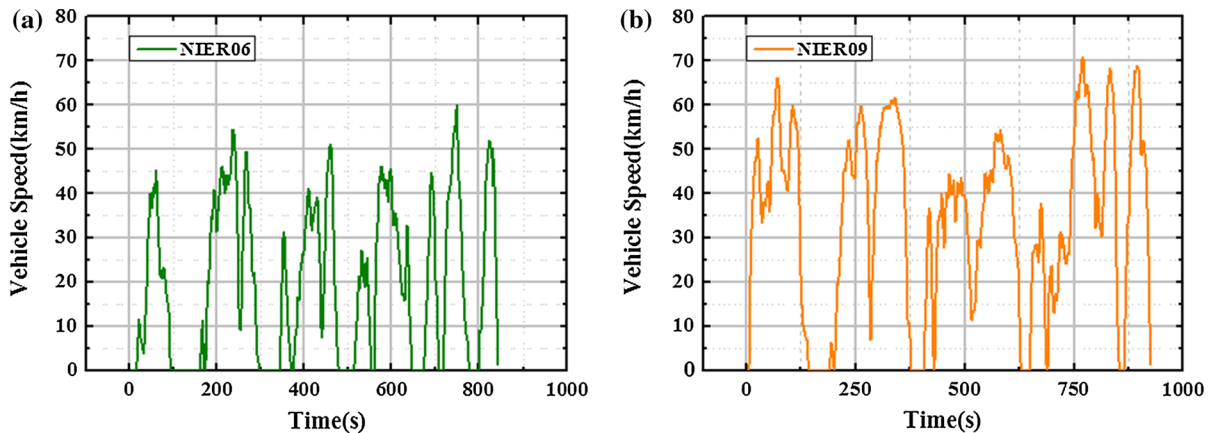
Fig. 1 City driving mode. **a** NIER 06 mode, **b** NIER 09 mode

The FTP-75 and NEDC certification test modes were tested in cold start conditions in order to compare the engine warm-up particle emissions. The particle emissions of urban driving conditions of the NIER modes were measured at hot start conditions.

Experimental apparatus and procedure

A schematic diagram of the experimental equipment used in this study is shown in Fig. 2. Particle emissions measured on a chassis dynamometer are diluted by the air passing through a high-efficiency particulate air (HEPA) at CVS tunnel. The diluted exhaust gas passes through a cyclone, which is used as a pre-classifier to remove the particles that are larger

than 2.5 micrometers in the CVS tunnel, and then the gravimetric method is used to measure the regulated PM. The PN measurement was conducted based on the European Particle Measurement Program (PMP). The PMP system consists of a volatile particle remover (VPR) and a condensation particle counter (CPC). The VPR removes volatile particles through heated primary dilution followed by evaporation in a heated tube. The particle emissions that pass through the VPR are counted by a CPC with a 50 % (D50) cut-off size of 23 nm.

The nanometer-sized particle emissions are measured by an engine exhaust particle sizer (EEPS 3090, TSI) at the tailpipes of the test vehicles in order to analyze the PN concentration and size distribution
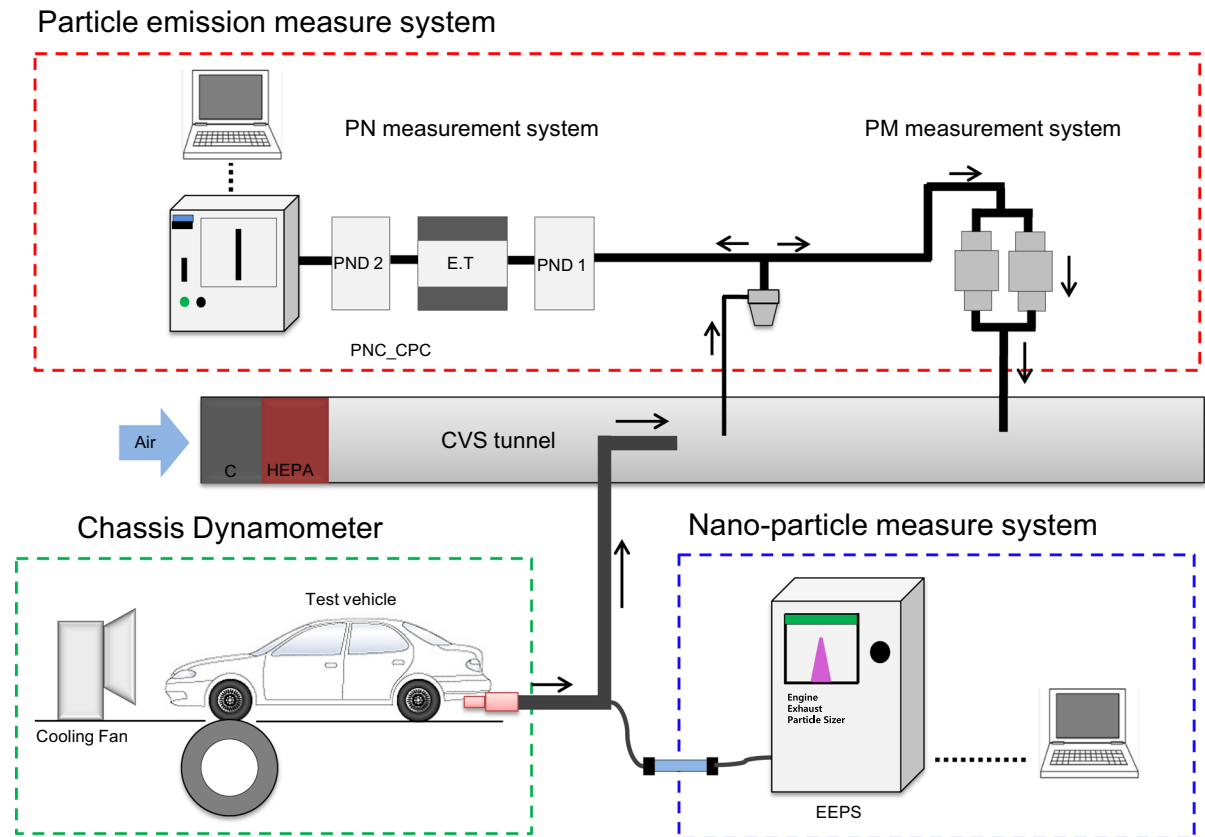
Fig. 2 Schematic diagram of vehicle test system.

characteristics in various driving modes. The EEPS spectrometer performs particle size classification based on differential electrical mobility classification. The charged aerosol enters the analyzer column near the on-axis and above the central rod. The particles are deflected radially toward the outer wall. The particle number concentration is determined by measuring the electrical current collected on a series of electrodes. The measurement range of the EEPS is from 5.6 to 560 nm, and it is possible to measure the particle size and PN distribution in real-time. A more detailed specification of the EEPS is presented in Table 4.

Results and discussion

Regulated particle emissions

Figure 3a represents the regulated PM in each phase and the weighted emissions of the test vehicles under the various driving modes. The green dotted line

Table 4 Specifications of EEPS equipment

Parameter	Change rate
Particle size range	5.6–560 nm
Concentration range	10^4–10^9 #/cm^3
Particle size resolution	32 Channels
Electrometer channels	22 Channels
Inlet cyclone 50 % cut-point	1 μm
Flow rates	Aerosol inlet: 10 L/min
	Sheath air: 40 L/min
Data averaging	0.1–60 s

indicates the Euro-6b current PM emission standard, and the orange dotted line indicates the LEV III current PM emission standard that will soon be implemented in the US. As shown in Fig. 3a, the PM emitted from PFI vehicles shows a significantly low value of less than 0.5 mg/km. On the other hand, the PM that was emitted from the GDI vehicles had a much higher value than the PM emitted from the PFI
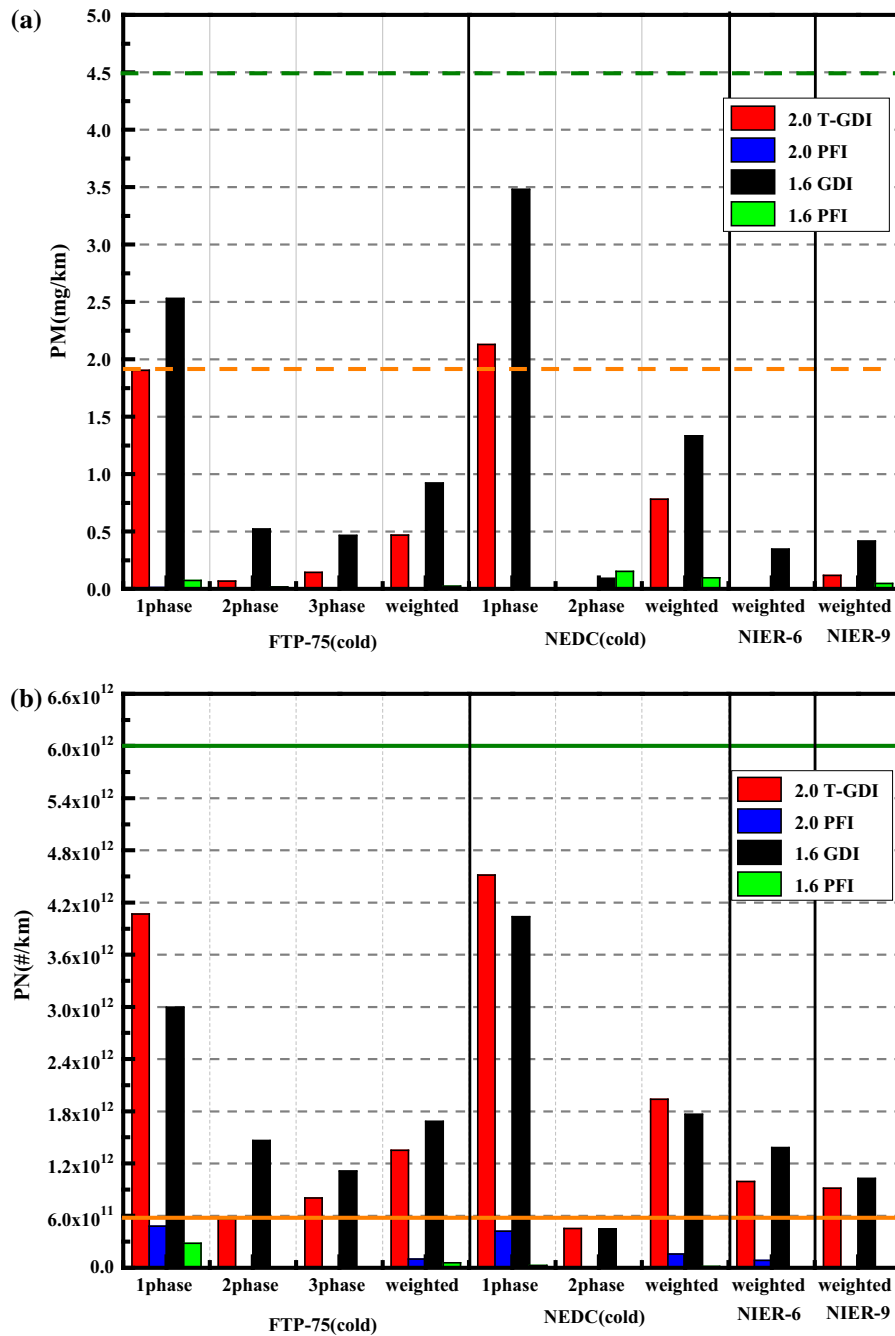
Fig. 3 Regulated particle emissions of test vehicles in the driving modes. **a** Particultae matter mass, **b** particle number

vehicles. When the PM is compared according to the driving mode, the PM of the FTP-75 and NEDC modes in cold start conditions was higher than the PM of the NIER06 and NIER09 modes in hot start conditions. In particular, weighted PM shows the highest values in

the NEDC modes because the NEDC mode includes the extra urban cycle of maximum speed 120 km/h. In the case of GDI vehicles, the results of the FTP-75 and NEDC modes in cold start conditions showed that the PM exceeded 2.0 mg/km in first phase of the cold

start, which does not satisfy the LEV III PM emission standard. However, after first phase, the PM was relatively low because the engine was sufficiently warmed up, and finally, the weighted PM satisfied the European and US regulations. The regulated PM for all vehicles in the NIER06 and NIER09 modes is below 0.5 mg/km because of a sufficient engine warm-up. In case of PFI vehicles, the results show low emissions levels that cannot be measured in all the test modes.

The regulated PN in each phase and the weighted PN of the test vehicles under the various driving modes are shown in Fig. 3b. The green line indicates the current European Euro-6b PN emission standard, and the orange line indicates the future Euro-6c PN emission standard that will be implemented in Europe. PFI vehicles have emitted the low PN emissions that can be ignored for all the driving modes. On the other hand, in the case of GDI vehicles, results show a relatively large number of PN emissions than PFI vehicles. Especially, PN emissions in first phase of FTP-75 and NEDC modes of cold start condition show a significantly higher value than the other phases and modes. Although there is reduction in PN emissions after the first phase, it still shows a lot of PN emissions than the PN emissions of the PFI vehicles. Due to hot start condition, PN emissions under the NIER06 and NIER09 are similar to result of the FTP-75 and NEDC modes after the first phase. As shown in Fig. 3b, similar to the PM results, the weighted PN emitted from PFI vehicles shows a low value and meets the PN emission standards of Euro-6b and Euro-6c in all driving modes. On the other hand, the weighted PN emitted from GDI vehicles is high. Although the regulated PN from GDI vehicles satisfied the EURO-6b emission standard, they did not meet the future EURO-6c emission standard, so it is necessary to find ways to reduce those emissions.

Particle emissions from test vehicles are closely related to the fuel injection system. Generally, particle emissions are formed in rich-burning region. In GDI system, most of the combustion is generated in the fuel-rich zones due to a difficulty to atomize the fuel and to form a homogeneous mixture. As well as poor fire often occur due to the fuel impingement close to the piston head and the cylinder wall. On the other hand, in the PFI system the fuel-rich zones are only located close to the intake valves. Therefore, the combustion in a GDI system is less complete, so more particles are emitted by GDI vehicles than by PFI vehicles. Also, engine temperature condition has a

significant effect on the particle emissions. Actually, in this study, most particles from the test vehicles are produced in the first phase of the cold start conditions of the FTP-75 and NEDC modes before the engine coolant and the combustion chamber temperature have reached a sufficiently warmed-up state. In particular, GDI vehicles required longer time for engine warm-up than the PFI vehicle due to the influence of the fuel direct injection in cylinder. Therefore, GDI vehicles emit more particle emissions for a long time than PFI vehicles.

Nanoparticle emission

Figure 4 shows the results obtained using the EEPS equipment to measure the nanometer-sized particles emitted from the test vehicles and the nanoparticle emissions according to the driving modes. Similar to the result of weighted PN in Fig. 3b, in the FTP-75 and NEDC modes of cold start conditions, the highest PN total concentration was observed, and the hot start conditions showed relatively low PN total concentration. The results show that there were more nanoparticle emissions from GDI vehicles than from PFI vehicles. Specifically, the nanoparticle emissions from PFI vehicles in the NIER06 and NIER09 hot start conditions were at such low levels that they were negligible. This result is believed to be due to the different fuel injection systems in the test vehicles.

The real-time PN concentrations measured with EEPS under the driving modes for one GDI vehicle (2.0 T-GDI) and one PFI vehicle (2.0 PFI) are presented in this section. Figure 5 shows the PN
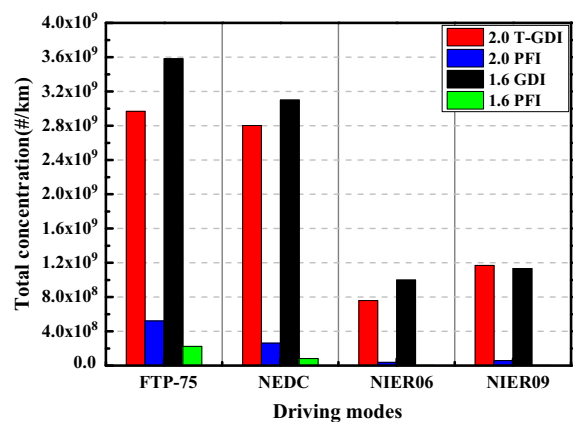

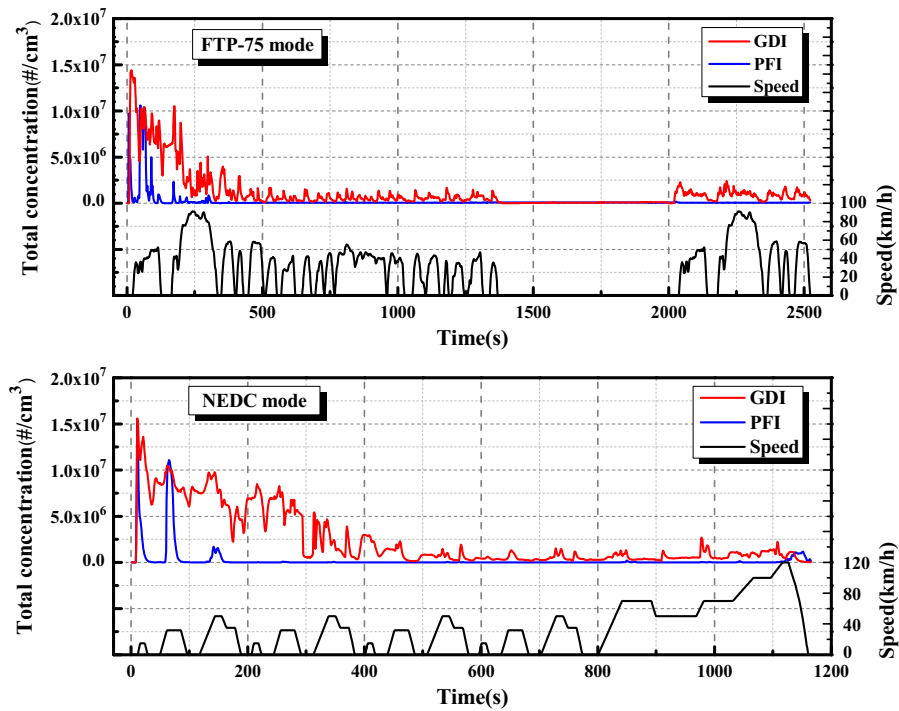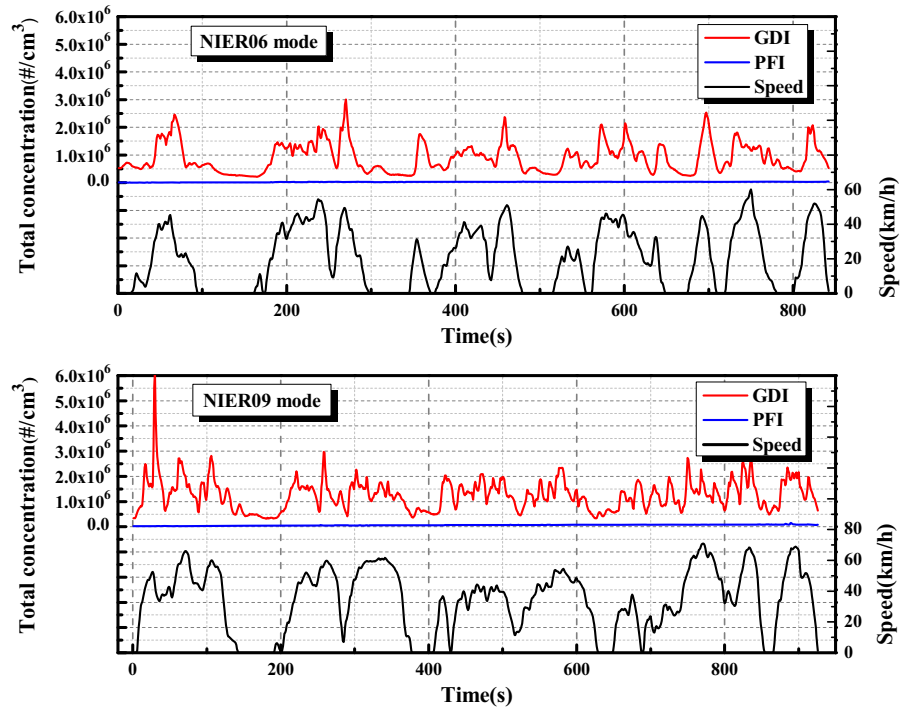**Fig. 4** Total concentration of nanoparticle emissions of test vehicle in the driving modes

Fig. 5 Time-resolved PN concentration and vehicle speed in the FTP-75 and NEDC modes

Fig. 6 Time-resolved PN concentration and vehicle speed in the NIER06 and NIER09 modes.
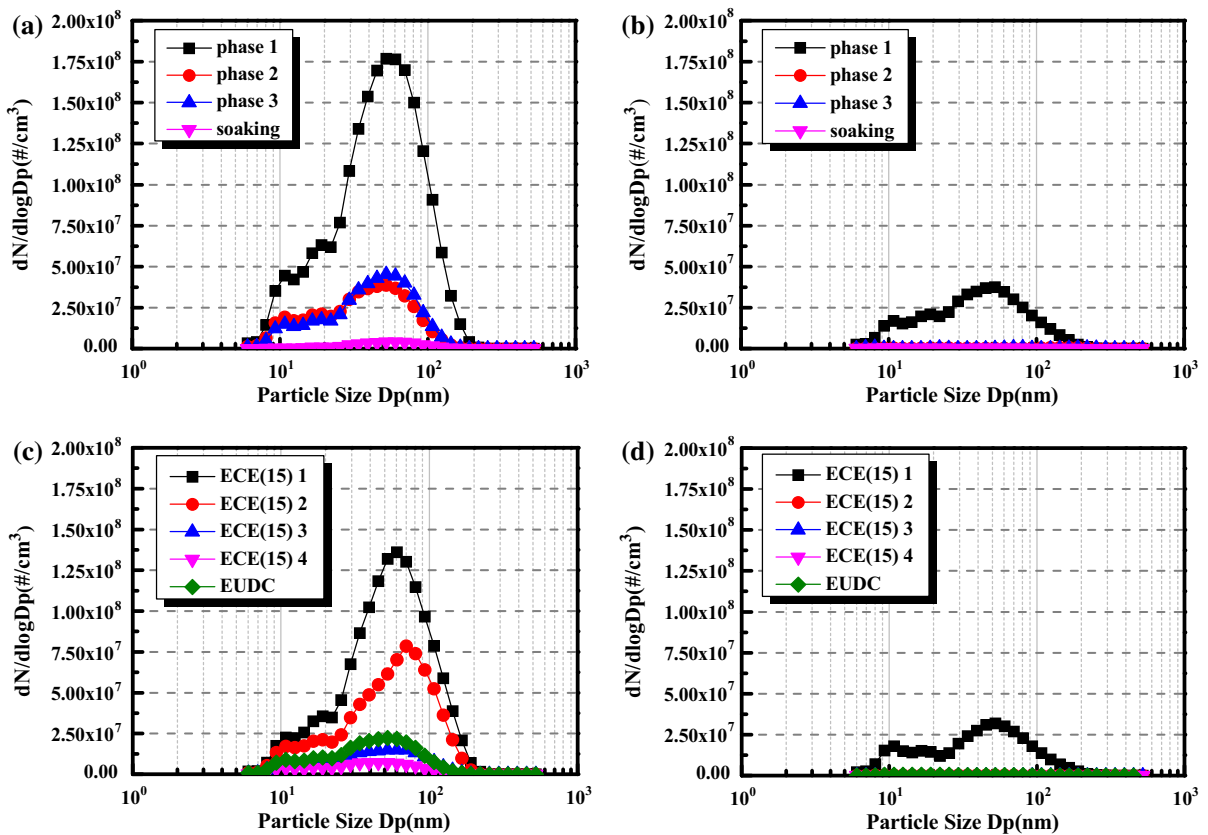
Fig. 7 PN distribution in each phase under the FTP-75 and NEDC modes. **a** PN distribution from GDI in FTP-75, **b** PN distribution from PFI in FTP-75, **c** PN distribution from GDI in NEDC, **d** PN distribution from PFI in NEDC

concentration in the cold start condition, and the PN concentration in the hot start condition is shown in Fig. 6. As shown in Fig. 5, in the cases of FTP-75 and NEDC, both GDI and PFI vehicles generate high PN concentrations at the first phase of a cold start since coolant temperature reached the sufficiently warm-up state. Especially, during cold start and high acceleration, peak value of PN of PFI vehicle is the same with GDI vehicle. When the fuel is injected from the port, a fuel film is generated on the intake valve surface and port wall. The fuel film cannot completely evaporate in the low coolant temperature and there is a part in the liquid state. This liquid fuel film generates a pool fire in the vicinity of the intake (Witze and Green 1997; Shin et al. 1994). As well as, during high acceleration, the large amount of fuel is injected in the intake port and its adhesion to the intake valve is increased. Therefore, the pool in the vicinity of the intake valve is increased and a lot of particle emission is discharged

(Merola et al. 2009; Tornatore et al. 2012). After the first phase, the PN concentration of the PFI vehicle decreased dramatically and then maintained a low value. However, the PN concentration increased again in the high-speed driving phase of 120 km/h in the NEDC mode. The PN concentration of the GDI vehicle also decreased after the first phase, but it stayed relatively high compared to the PN concentration of the PFI vehicle. By comparing first phase of the cold start and third phase of the hot start in FTP-75, the PN concentrations of the GDI and PFI vehicles had a notable difference. In the case of the GDI vehicle, regardless of the speed, there was a high PN concentration for approximately 250 s after the start driving mode. In third phase, however, the PN concentration showed a similar trend to the speed profile of the driving mode. The PN concentrations of the PFI vehicle were also high during the cold start, but for a shorter time than for the GDI vehicle. The result of PFI
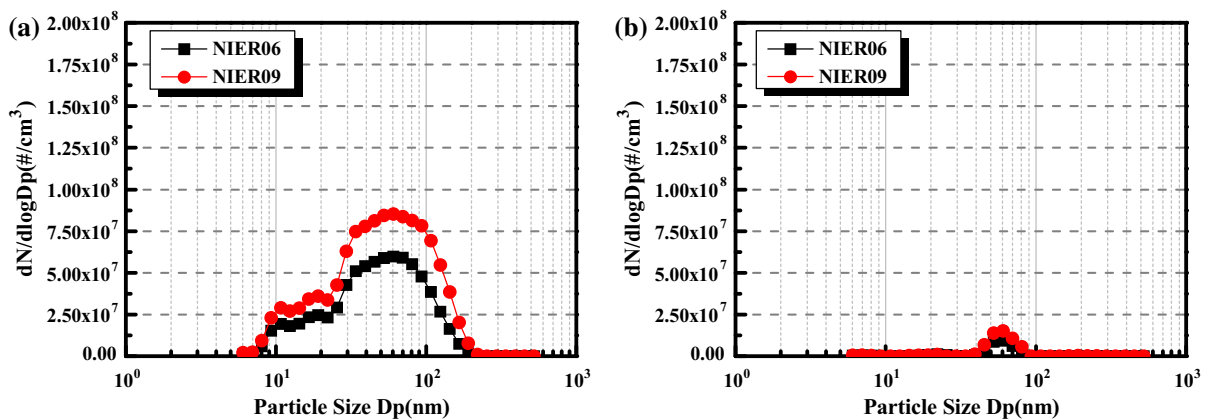
Fig. 8 PN distribution in each phase under the NIER06 and NIER09 modes. **a** PN distribution from GDI in NIER, **b** PN distribution from PFI in NIER

vehicle in third phase shows that a low level of emissions may be ignored. These results can be seen in the NEDC mode trend. For NIER06 and NIER09, the PN concentrations have low values. It is similar to the results for FTP-75 and NEDC after the first phase. Also, the PN concentration is low for the PFI vehicle, and the PN concentration of the GDI vehicle is similar to the speed profile of the driving mode.

Particle size distribution

This chapter shows the particulate size distributions emitted from GDI and PFI vehicles in each phase under the FTP-75 and NEDC modes. As shown in Fig. 7, the results for the test vehicles under the FTP-75 and NEDC modes indicate that the nanoparticles are mostly emitted at around 50 nm. In FTP-75 mode, phases 2 and 3, except for the soaking phase of the engine off condition, have similar particle size distributions and values. In the NEDC mode, while driving the ECE 15 phases of the urban driving pattern repeated four times, the nanoparticle emissions decreased gradually. However, in the EUDC phase of the extra urban driving pattern, more nanoparticle emissions were emitted than from the third and fourth ECE 15 phases. Since the EUDC driving phase includes high-speed driving at 120 km/h, more fuel is injected than in other phases. In addition, the precision fuel injection fails and wall wetting occurs in the engine combustion chamber. For this reason, the combustion was less complete, so the nanoparticle emissions increased. On the other hand, the results for

the PFI vehicle showed that except in the first phase of the cold start condition, the nanoparticle emissions were at such low levels that they were within the error range of the EEPS equipment. Figure 8 shows the particulate size distributions emitted from GDI and PFI vehicles under the NIER06 and NIER09 modes of the hot start condition. The result shows similar particle size distributions and values for the FTP-75 and NEDC modes after the first phase.

Influences of vehicle driving pattern

The influence of the vehicle driving pattern on the size distribution was determined by dividing the four kinds of driving patterns of the vehicle and analyzing the data. The percentage of the driving pattern in each mode is shown in Table 3. Figure 9 shows the nanoparticle emissions according to the driving patterns of the GDI and PFI vehicles in the FTP-75 and NEDC modes. Result of the GDI vehicle in both driving modes shows the most nanoparticle emissions at around 50 nm during acceleration. The acceleration increases the amount of fuel injected since the throttle opening is increased (Li et al. 2013), so there is a locally richer mixture in the combustion chamber. For this reason, acceleration generates more particle emissions. In the FTP-75 mode, the deceleration following the acceleration also shows a large number of emissions. In other words, when the speed is changed, nanoparticle emissions are high. However, the result of the NEDC mode shows the second highest nanoparticle emissions in the cruising pattern. The difference in the results is believed to occur
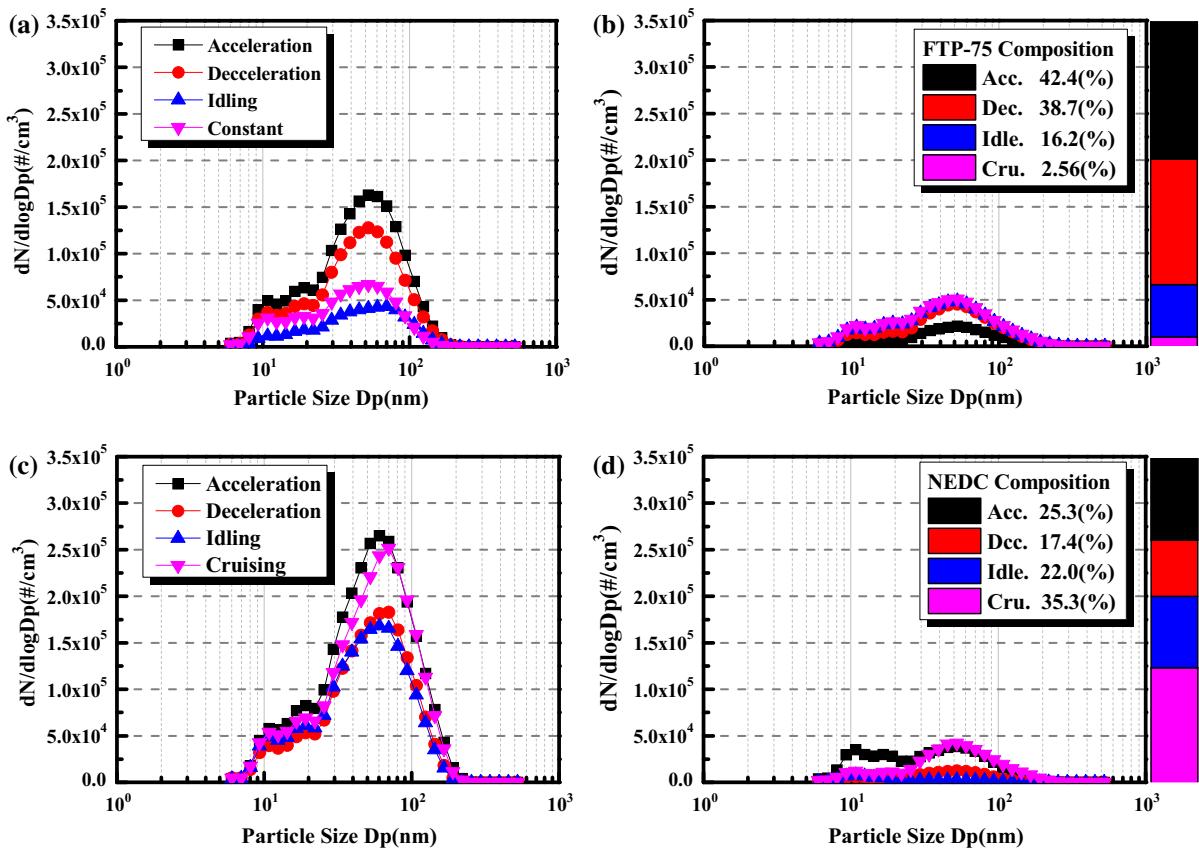
Fig. 9 PN distribution in different driving patterns under the FTP-75 and NEDC modes. **a** PN distribution from GDI in FTP-75, **b** PN distribution from PFI in FTP-75, **c** PN distribution from GDI in NEDC, **d** PN distribution from PFI in NEDC

Table 5 The proportions of vehicle driving patterns

	FTP-75		NEDC		NIER06		NIER09	
	s	%	s	%	s	%	s	%
Acceleration	795	42.42	299	25.34	314	37.29	402	43.41
Deceleration	726	38.74	205	17.37	312	37.05	416	44.92
Idling	305	16.27	260	22.03	216	25.65	108	11.66
Cruising	48	2.56	416	35.25	0	0.00	0	0.00
Total	1874	100.00	1180	100.00	842	100.00	926	100.00

due to the pattern difference in the running mode. As shown in Table 5, in the FTP-75 mode, the percentages of acceleration and deceleration were the highest at 42.4 and 38.7 %, respectively, except for the soaking of the idling pattern. On the other hand, in the NEDC mode, since 35.3 % of the mode is the cruising pattern, the nanoparticle emissions are high. In the case of the PFI vehicle, the results do not vary significantly according to the driving pattern, and all cases show very low nanoparticle emissions. Figure 10 shows the nanoparticle distribution according to the driving pattern in the NIER06 and NIER09 hot start conditions. Although the nanoparticle emissions from the PFI vehicle are low enough to be within the measurement error range, the emissions from the GDI vehicle are relatively high during acceleration and deceleration.
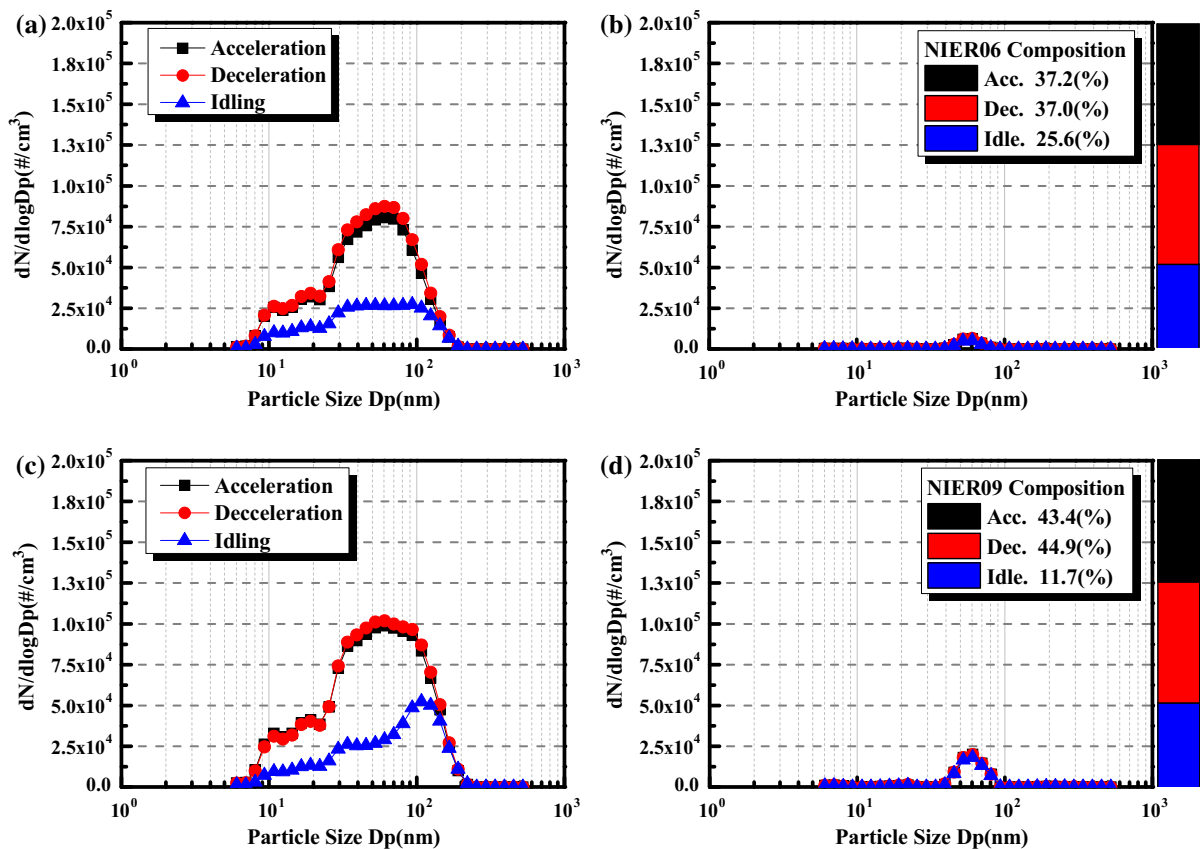
Fig. 10 PN distribution in different driving patterns under the NIER06 and NIER09 modes. **a** PN distribution from GDI in NIER06, **b** PN distribution from PFI in NIER06, **c** PN distribution from GDI in NIER09, **d** PN distribution from PFI in NIER09

Conclusions

A total of 4 types of passenger vehicles equipped with gasoline direct injection and port fuel injection engines have been tested for particle emissions in various driving modes. Of the four vehicles tested, one type of GDI vehicle and one type of PFI vehicle are selected in order to compare the nanoparticle emissions. The following are the summary and conclusions of the study:

The PM emissions of the PFI vehicles were less than 0.5 mg/km, and the GDI vehicles had more PM emissions than PFI vehicles. However, all of the test vehicles meet the European and U.S. PM emission standards. On the other hand, while the PFI vehicles had only a small amount of PN emissions, the PN emissions of the GDI vehicles do not meet the EURO-6c emission standard that will be implemented in Europe.

The total number of nanoparticles measured by the EEPS equipment, like the release of regulated particle

emissions, was higher in the FTP-75 and NEDC modes of the cold start condition. Also, the real-time PN concentration was measured by the EEPS. A comparison of the GDI and PFI nanoparticle emissions showed that the direct injection of fuel in the cylinder generated more particle emissions than a conventional port fuel system. In the temperature condition, irrespective of the fuel injection system, both show a number of emissions from the cold start condition.

The distribution of nano- particle emissions according to size was measured in each phase. The highest particle sizes of the total concentration for the test vehicles were similar, ranging from 50 to 70 nm. In addition, the total concentration of nanoparticles tended to gradually decrease from the first phase to the last phase. However, in the NEDC mode, the total concentration was increased again in the EUDC extra urban driving phase.

This study compared the nanoparticle emission characteristics according to the driving pattern. While

most of the driving mode is high in acceleration and deceleration of the PN emissions, the high PN in acceleration and pattern of cruising is confirmed in the NEDC mode. This is determined to be a result of the differences in the driving mode patterns.

Consequently, in this study, GDI vehicle was confirmed to exhibit much higher particle emissions than PFI vehicles in various driving conditions, and a continuous study of the particle emissions and reduction in GDI vehicles is necessary in the future.

References

Andersson J, Giechaskiel B, Muñoz-Bueno R, Sandbach E, Dilara P (2007) Particle measurement programme (PMP) light-duty inter-laboratory correlation exercise (ILCE_LD) final report. European Commission Joint Research Centre Institute for Environment and Sustainability

Arsie I, Di Iorio S, Vaccaro S (2011) Experimental characterization of nanoparticles emissions in a port fuel injection spark ignition engine. SAE Technical Paper. doi:10.4271/2011-24-0208

Bonandrini G, Di Gioia R, Papaleo D, Venturoli L (2012) Numerical study on multiple injection strategies in DISI engines for particulate emission control. SAE Technical Pap. doi:10.4271/2012-01-0400

Bonatesta F, Chiappetta E, La Rocca A (2014) Part-load particulate matter from a GDI engine and the connection with combustion characteristics. Appl Energy 124:366–376. doi:10.1016/j.apenergy.2014.03.030

Braisher M, Stone R, Price P (2010) Particle number emissions from a range of European vehicles. SAE Technical Paper. doi:10.4271/2010-01-0786

Brehob DD, Fleming JE, Haghgooie M, Stein RA (1998) Stratified-charge engine fuel economy and emission characteristics. SAE Technical Paper. doi:10.4271/982704

Brugge D, Durant JL, Rioux C (2007) Near-highway pollutants in motor vehicle exhaust: a review of epidemiologic evidence of cardiac and pulmonary health risks. Environ Health 6:23. doi:10.1186/1476-069X-6-23

Cavina N, Businaro A, Moro D, Di Gioia R, Bonandrini G, Papaleo D, Picerno M (2015) Assessment of the influence of GDI injection system parameters on soot emission and combustion stability through a numerical and experimental approach. SAE Int J Engines. doi:10.4271/2015-24-2422

Donaldson K, Stone V, Gilmour PS, Brown DM, MacNee W (2000) Ultrafine particles: mechanisms of lung injury. R Sco Lond Math Phys Eng Sci. doi:10.1098/rsta.2000.0681

(EC) R (No 715/2007) (2007) On type approval of motor vehicles with respect to emissions from light passenger and commercial vehicles (Euro 5 and Euro 6) and on access to vehicle repair and maintenance information

Fu H, Wang Y, Li X, Shuai S-J (2014) Impacts of cold-start and gasoline RON on particulate emission from vehicles powered by GDI and PFI engines. SAE Technical Paper. doi:10.4271/2014-01-2836

Kayes D, Hochgreb S (1998) Investigation of the dilution process for measurement of particulate matter from spark-ignition engines. SAE Technical Paper. doi:10.4271/982601

Kim J, Choi K, Myung C-L, Lee Y, Park S (2013) Comparative investigation of regulated emissions and nano-particle characteristics of light duty vehicles using various fuels for the FTP-75 and the NEDC mode. Fuel 106:335–343. doi:10.1016/j.fuel.2012.12.047

Künzli N et al (2000) Public-health impact of outdoor and traffic-related air pollution: a European assessment. The Lancet 356:795–801. doi:10.1016/S0140-6736(00)02653-2

Lee KW, Yeom DJ (2012) Establishment of an installation process of a valve seat to a cylinder head using the cae technique. Int J Automot Technol 13:687–692. doi:10.1007/s12239-012-0067-7

Li T, Chen X, Yan Z (2013) Comparison of fine particles emissions of light-duty gasoline vehicles from chassis dynamometer tests and on-road measurements. Atmos Environ 68:82–91. doi:10.1016/j.atmosenv.2012.11.031

Luijten B, Adomeit P, Brunn A, Somers B (2013) Experimental investigation of in-cylinder wall wetting in GDI engines using a shadowgraphy method. SAE Technical paper. doi:10.4271/2013-01-1604

Maricq MM, Podsiadlik DH, Chase RE (1999) Examination of the size-resolved and transient nature of motor vehicle particle emissions. Environ Sci Technol 33:1618–1626. doi:10.1021/es9808806

Merola SS, Sementa P, Tornatore C, Vaglieco BM (2009) Spectroscopic investigations and high resolution visualization of the combustion phenomena in a boosted PFI SI engine. SAE Int J Engines 1:1617–1629. doi:10.4271/2009-01-1814

Nel A, Xia T, Mädler L, Li N (2006) Toxic potential of materials at the nanolevel. Science 311:622–627. doi:10.1126/science.1114397

Pesiridis A (2012) Issues in the integration of active control turbochargers with internal combustion engines. Int J Automot Technol 13:873–884. doi:10.1007/s12239-012-0088-2

Price P, Stone R, OudeNijeweme D, Chen X (2007) Cold start particulate emissions from a second generation DI gasoline engine. SAE Technical Paper. doi:10.4271/2007-01-1931

Rubino L, Phillips PR, Twigg MV (2005) Measurements of ultrafine particle number emissions from a light-duty diesel engine using SMPS, DMS, ELPI and EEPS. SAE Technical Paper. doi: 10.4271/2005-24-015

Sementa P, Vaglieco BM, Catapano F (2012) Thermodynamic and optical characterizations of a high performance GDI engine operating in homogeneous and stratified charge mixture conditions fueled with gasoline and bio-ethanol. Fuel 96:204–219. doi:10.1016/j.fuel.2011.12.068

Shin Y, Cheng WK, Heywood JB (1994) Liquid gasoline behavior in the engine cylinder of a SI engine. SAE Technical Paper. doi:10.4271/941872

Tong K, Quay BD, Zello JV, Santavicca DA (2001) Fuel volatility effects on mixture preparation and performance in a GDI engine during cold start. SAE Technical Paper. doi:10.4271/2001-01-3650

Tornatore C, Marchitto L, Valentino G, Corcione FE, Merola SS (2012) Optical diagnostics of the combustion process in a PFI SI boosted engine fueled with butanol-gasoline blend. Energy 45:277–287. doi:10.1016/j.energy.2012.03.006

Witze P, Green RM (1997) LIF and flame-emission imaging of liquid fuel films and pool fires in an SI engine during a simulated cold start. SAE Technical Paper. doi:10.4271/970866

Zhang S, McMahon W (2012) Particulate emissions for LEV II light-duty gasoline direct injection vehicles. SAE Int J Fuels Lubr 5:637–646. doi:10.4271/2012-01-0442

Zhao F, Lai MC, Harrington DL (1999) Automotive spark-ignited direct-injection gasoline engines. Prog Energy Combust Sci 25:437–562. doi:10.1016/s0360-1285(99)00004-0